Journal of
Bioremediation & Biodegradation

Zakaria, et al. J Bioremed Biodeg 2013, S4
DOI: 10.4172/2155-6199.S4-001

Research Article Open Access

Characterization of Fe_2O_3/FeOOH Catalyzed Solvolytic Liquefaction of Oil Palm Empty Fruit Bunch (EFB) Products

Sarani Zakaria[1]*, Tze Khong Liew[1], Chin Hua Chia[1], Fei Ling Pua[1], Fan Suet Pin[1], Rasidi Roslan[1], Umar Adli Amran[1], Antje Potthast[2], Thomas Rosenau[2] and Falk Liebner[2]

[1]*School of Applied Physics, Faculty of Science and Technology, Universiti Kebangsaan Malaysia (UKM), 43600 UKM, Bangi, Selangor, Malaysia*
[2]*Department of Chemistry, University of Natural Resources and Applied Life Sciences, (BOKU) A-1190, Vienna, Austria*

Abstract

The addition of Fe_2O_3/FeOOH nanoparticles as a catalyst in solvolytic liquefaction of oil palm empty fruit bunch (EFB) could be cheaper and efficient alternative for biomass industry in Malaysia. Fe_2O_3/FeOOH can be found naturally in limonite ores and it is cheap, but work efficiently in catalyzing liquefaction. The purpose of this study is to understand the effects on the combination of Fe_2O_3/FeOOH, as the catalyst in solvolytic liquefaction of EFB. Solvolytic liquefaction of EFB fiber, with and without Fe_2O_3/FeOOH, was carried out in the nitrogen gas atmosphere using an autoclave. This liquefaction mainly yielded solvolytic oil, n-hexane insoluble preasphaltene and asphaltene phase (PA+A), and solid residue. The presence of catalyst has significantly increased the liquefaction yield and solvolytic oil fraction. Chemical elemental analysis has showed that the products with lower oxygen content are obtained when Fe_2O_3/FeOOH is used. FT-IR spectroscopy proved that the conversion of the higher molecular compound to the lower molecular compounds with larger number of functional groups has occurred. The analytical Pyrolysis-GCMS revealed the existence of lower molecular weight alcohols, ketones, phenolic and aromatic compounds.

Keywords: Biomass; Catalyst, Empty fruit bunch; Solvolysis; Liquefaction

Introduction

Oil palm industries in Malaysia generate about 90 million tons of renewable biomass per year. Oil palm biomasses include oil palm trunks, pruned and felled fronds, shells, palm press fiber and Empty Fruit Bunches (EFB). EFB is a suitable renewable biomass material for the conversion into the valuable products, because it is locally abundant and rich in lingo cellulosic components [1].

Biomass can be converted into useful chemicals and liquid fuels *via* thermo chemical conversion processes, including combustion, gasification, pyrolysis, liquefaction and carbonization. Among them, liquefaction is a promising way to provide either valuable chemicals or liquid fuels [2]. Solvolytic liquefaction has been intensively studied in recent years, as a method that allowed the production of useful polymer precursors or chemicals by chemical treatment of biomass, in the presence of specific organic solvents (media). Depending on both, the type of biomass and the reaction conditions, different products can be obtained [3].

Metallic catalysts are known to be effective additives in direct coal and biomass liquefaction. Previous studies [4-8] showed that the addition of catalysts can greatly improve the conversion rates and yield, and affect the composition of the liquid product. Biomass liquefaction, using Fe_2O_3 as a catalyst, is a common method to produce liquid fuel and useful chemicals, and also effective in improving the yield of biomass conversion [5,9,10]. FeOOH catalyst was also applied in the coal liquefaction, with high yield of conversion and high catalytic activity observed from previous studies [11,12]. Combination of Fe_2O_3 and FeOOH catalysts obtained from natural resources of limonite ores for coal liquefaction was studied by Kaneko et al. [13], showed high liquefaction activity and excellent oil yield from the process.

This paper reports on the effects of using Fe_2O_3/FeOOH nanoparticles on the yield and composition of the solvolytic oil obtained from oil palm Empty Fruit Bunches (EFB), through solvolytic liquefaction. Instead of the commonly used phenol, ethylene glycol (EG) was used as a solvent, because it is less harmful [14]. Nanoparticles size of Fe_2O_3/FeOOH is used to increase the dispersion and optimize the activity of these catalysts [15].

Materials and Methods

EFB fiber was supplied by Szetech Engineering Sdn. Bhd. The average fiber size is about 0.8 mm in dimension. The properties of EFB fiber are shown in Table 1. Ferric chloride ($FeCl_3$) and sodium hydroxide (NaOH) were purchased from Sigma-Aldrich and used as received.

The loading of the Fe_2O_3/FeOOH catalyst onto the EFB fibers was accomplished by the *in-situ* synthesis, as reported earlier [16]. Distilled water (100 ml) were filled into a round bottom flask, heated to 90°C and purged with nitrogen gas. EFB fiber (5 g) was then added into the flask and agitated using mechanical stirrer at 600 rpm. $FeCl_3$ (0.305 g) were added to the suspension, and agitation was continued for another 5 minutes for Fe^{3+} ions to disperse thoroughly in the suspension. Subsequently, 5.75 ml of an aqueous NaOH solution (0.023 moles) were added to the fiber suspension to form the Fe_2O_3/FeOOH. After washed with acetone and distilled water, the fiber suspension was filtered and dried at 105°C for 24 hours. EFB and EG (mass ratio of 4:1) were placed into a 200 ml autoclave equipped with stirring and heating systems. After purging with nitrogen gas, the autoclave was then heated to 250°C, followed by a reaction time of 60 minutes. After the

***Corresponding author:** Sarani Zakaria, School of Applied Physics, Faculty of Science and Technology, Universiti Kebangsaan Malaysia (UKM), 43600 UKM, Bangi, Selangor, Malaysia, Tel: +60 3 8921 3261; Fax: +60 3 8921 3777; E-mail: sarani@ukm.my

Received April 09, 2013; **Accepted** June 12, 2013; **Published** June 14, 2013

Citation: Zakaria S, Liew TK, Chia CH, Pua FL, Pin FS, et al. (2013) Characterization of Fe_2O_3/FeOOH Catalyzed Solvolytic Liquefaction of Oil Palm Empty Fruit Bunch (EFB) Products. J Bioremed Biodeg S4: 001. doi:10.4172/2155-6199.S4-001

Component/Property	Measured Value	Method
Proximate analysis		
Moisture	10.40	ASTM E871
Ash	3.60	ASTM D 1102-84
Volatile matters	77.50	ASTM E872
Fixed carbon	18.90	By difference
Chemical Properties		
Elemental analysis		
Carbon	45.01	CHNS Analyzer
Hydrogen	8.35	
Nitrogen	0.09	
Sulphur	0.00	
Oxygen	46.55	By difference
Chemical composition		
Holocellulose	76.54	ASTM D 1104-56
Alphacellulose	49.30	ASTM D 1103-60
Klason lignin	16.23	ASTM D 1106-56
Extratives (Alcohol-toluene soluble)	3.29	ASTM D 1107-56
Extratives (Hot water soluble)	5.82	ASTM 1110-56

Table 1: Proximate and ultimate properties of EFB (wt %).

reaction completed, the autoclave was allowed to cool down to room temperature. Both liquid and solid products were collected for further analyses. The liquid product was separated into two fractions: Those soluble in THF, but insoluble in n-hexane, are referred to preasphaltene and asphaltene (PA+A), while oil is referred to those which are soluble in both solvents. Oil is later known as solvolytic oil fraction. Figure 1 shows the flowchart of solvolytic liquefaction process carried out in this study. The residue fraction is referred to those which do not dissolved in the solvents.

The total conversion and the yield of solvolytic oil, PA+A and residue fractions obtained in the solvolytic liquefaction reaction were calculated according to following equations:

$$X\% = (1-W_s/W_0)\times 100\% \quad (1)$$

$$PA+A\% = (W_a/W_0)\times 100\% \quad (2)$$

$$O+G\% = [X-(PA+A)]\times 100\% \quad (3)$$

where X is total conversion of EFB, O+G is the total yield of solvolytic oil and gas fractions, W_s is the dry weight of residue, W_a is the dry weight of PA+A, and W_0 is the dry weight of EFB.

C, H, N and S contents of oil products were determined using Thermo Finnigan Eager-300 CHNS analyzer. Oxygen content was estimated based on the difference of C, H, N and S contents of the samples. The HHV of the oil products was then calculated using the Dulong formula developed by Demirbas [17], as followed:

$$HHV\ (MJ/kg) = \{33.5[C]+142.3[H]-15.4[O]-14.5[N]\}\times 10^{-2} \quad (4)$$

The samples for FT-IR were prepared with equal sample weight mix with KBr, to form pellets. The samples were recorded using a Perkin-Elmer FTIR2000 spectrophotometer in the near IR region (4000-370 cm^{-1}).

Curie point pyrolysis GC/MS was performed using a Pyromat (GSG Ltd.), coupled with a GC 6890 and MSD 5973 (Agilent Technologies). About 200 µg of the sample had undergone pyrolysis at 600°C (FecralloyTM) for 10 seconds. The pyrolysate was carried by helium into the inlet (250°C, split 1: 20) of the gas chromatograph. Separation was achieved using a fused silica column (DB-5 ms, 30 m, 0.25 mm, 25 µm), a column flow of 0.9 ml min^{-1}, an oven programmed starting with 50°C (5 min), then 5°C min^{-1} to 280°C (2 min), and an auxiliary temperature of 250°C. The mass spectrometer was operated in EI mode at 70 eV, 230°C, and 1.5×10^{-5} Torr.

Results and Discussion

Figure 2 shows the total conversion and yield of the solvolytic liquefaction of EFB, with and without Fe_2O_3/FeOOH. As shown in Figure 2, the total conversion of EFB liquefaction increase from 44.26% to 65.58%, when Fe_2O_3/FeOOH presence in fiber. The same trend can be observed for the yield of O+G. In the presence of catalysts, the yield of O+G obtain is 51.40%. If compared to the sample without catalysts, the yield of O+G is lowered by 15.36%. The yield of PA+A has also increased from 8.22% to 14.18%, in the presence of Fe_2O_3/FeOOH. From the results, we can conclude that the presence of Fe_2O_3/FeOOH as catalyst in the solvolytic liquefaction of EFB has significantly enhanced the bond cleavage, cracking and thermal degradation of the fiber.

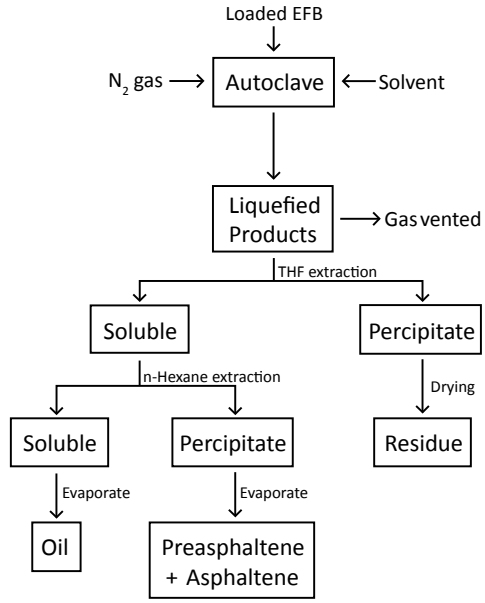

Figure 1: Diagram of solvolytic liquefaction process.

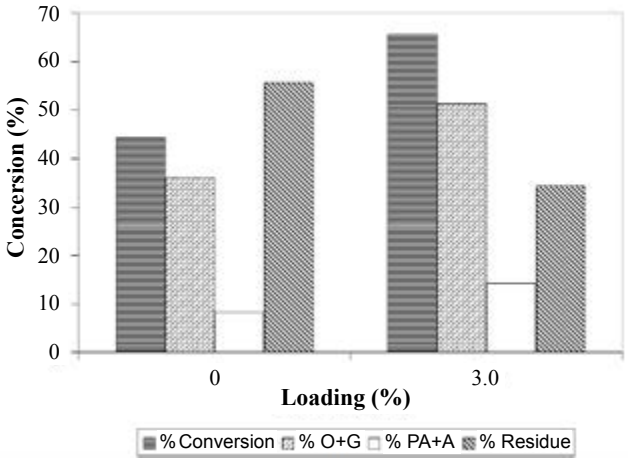

Figure 2: Conversion and yield of liquefaction of EFB with and without FeOOH/Fe_2O_3 loading. Condition: 250°C, 60 min and N_2 gas.

Table 2 shows the results of elemental analysis and the Higher Heating Values (HHV) of different product fractions from both catalytic and non-catalytic liquefaction process. In the absence of catalyst, preasphaltene/asphaltene fraction (PA+A) is found to have the highest carbon and the lowest oxygen content from all product fractions that resulting in the highest HHV value. Meanwhile, solvolytic oil fraction contains the least carbon and highest oxygen. Hence, its HHV value is slightly higher than the residue. This is probably due to the higher content of hydrogen. However, the HHV of these two fractions (solvolytic oil and residue) are very low, because of the unfavorable C/O ratio. The presence of the Fe_2O_3/FeOOH catalyst during solvolytic liquefaction only resulted to slightly increases of carbon contents and HHV values of these fractions, but has a comparatively strong effect on the PA+A fraction.

Figure 3 compares the IR spectra of EFB fiber (a) and the solvolytic oil fraction (b) obtained from catalytic liquefaction using ethylene glycol, as reacting/heat transferring medium. The vibration band pattern of spectrum 3(a) is similar to that of woody biomass [18], and

	Without Catalyst			With Catalyst		
Element	Oil	PA+A	Residue	Oil	PA+A	Residue
Carbon	33.278	66.326	40.852	35.226	80.010	43.150
Hydrogen	7.432	5.805	5.018	8.395	6.340	5.196
Nitrogen	0.522	1.635	0.333	0.000	1.289	0.129
Sulfur	0.000	0.000	0.000	0.000	0.000	0.000
Oxygen	58.768	26.234	53.797	56.378	12.362	51.525
HHV (MJ/kg)	**12.598**	**26.202**	**12.493**	**15.065**	**33.734**	**13.896**

Table 2: Elemental contents and higher heating values (HHV) of the different product fractions obtained by liquefaction, without and in the presence of Fe_2O_3/FeOOH nanoparticles.

contains typical signals of cellulose, hemicelluloses and lignin. The presence of cellulose is confirmed by the characteristic bands such as O-H stretching (3428 cm^{-1}), C-H_2 shearing (1437 cm^{-1}), C-H stretching (1376 cm^{-1}), O-H in-plane bending (1330 cm^{-1}), C-O-C asymmetry stretching (1162 cm^{-1}) and C-O stretching (1050 cm^{-1} and 1020 cm^{-1}). Typical signals reducing end group for hemicellulose and cellulose can be found at 1734 cm^{-1} (carbonyl C=O stretching), 1376 cm^{-1} (C-H stretching), 1162 cm^{-1} (C-O-C asymmetry stretching), 1050 cm^{-1} (C-O stretching) and 1020 cm^{-1} (C-O stretching). These bands caused by aromatic C=C stretching (1631 cm^{-1} and 1505 cm^{-1}), C-H_2 bending (1437 cm^{-1}), aromatic in-plane C-H deformation (1256 cm^{-1}), and C-H in-plane bending (891 cm^{-1}) are strongly indicative for the presence of lignin in the EFB fibers. Table 3 and 4 summarized the FTIR bands and functional groups assignment of EFB fiber and solvolytic oil fractions, respectively.

The IR spectrum of the oil fraction is presented in Figure 3b. The broad stretching band of hydroxyl groups (3600-3200 cm^{-1}) is assumed to be due to the presence of considerable amounts of non reacted ethylene glycol, EG oligomers and EG derivatives, a distinctly increased number of hydroxyl groups in lower molecular compounds obtained from the EFB fibers by thermal hydrocracking, and residual amounts of water (Table 4). The intensity of C-H stretching (3000 to 2800 cm^{-1}) and C-H bending (1465 to 1350 cm^{-1}) bands increase as more alkane groups formed from the liquefaction reaction. The formation of carbonyl compounds (carboxylic acids, ketones and aldehydes, e.g.) due to the decomposition of cellulose and hemicellulose is shown by peaks at 1730 to 1650 cm^{-1} (increased intensity of C=O stretching). The bands appearing in the range of 1300 to 950 cm^{-1} can be assigned to C-O stretching and O-H bending, indicating the presence of primary, secondary and tertiary alcohols, phenols, esters and ethers. The sharp

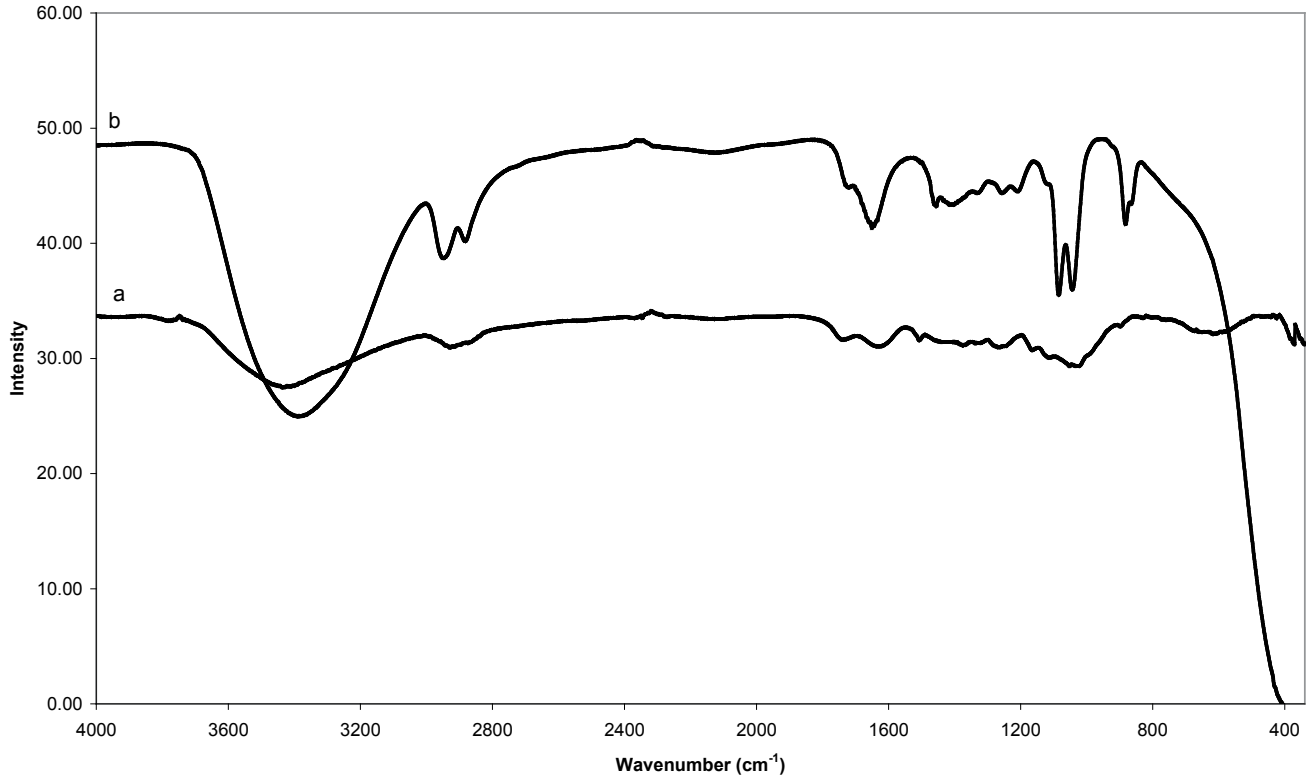

Figure 3: FTIR spectrum of EFB fiber (a) and oil product (b).

signal at 1080 cm^{-1} and 1040 cm^{-1} are most likely due to C-O stretching confirming the presence of alcohols and ethers, as they are also detected in the analytical pyrolysis of GC/MS. Furthermore, the appearance of signals that could be clearly attributed to the presence of aromatic (1460 cm^{-1}, 1240 cm^{-1}, 1120 cm^{-1} and 870 cm^{-1}), and carbonyl groups (1720 cm^{-1}) indicate that the oil fraction contains a certain percentage of lignin derived decomposition products.

Figure 4 and 5 show the gas chromatograms of the solvolytic oil fractions obtain through the liquefaction process, with and without

Bands (cm^{-1})	Functional group
3428	O-H stretching
2927	C-H, $C-H_2$ stretching
1734	Carbonyl C=O stretching (hemicellulose)
1631	C=C stretching (lignin)
1505	Benzene ring stretching (lignin)
1437	$C-H_2$ shearing(cellulose), $C-H_2$ benching (lignin)
1376	C-H benching(cellulose, hemicellulose)
1330	O-H in-plane benching (cellulose)
1256	C-O-C stretching in alkyl aromatic (lignin)
1162	C-O-C asymmetry stretching (cellulose, hemicellulose)
1050	C-O stretching (cellulose, hemicellulose)
1020	C-O stretching (cellulose, hemicellulose)
891	C-H in-plane benching (lignin)

Table 3: FTIR bands and functional groups assignment of EFB fiber.

Bands range (cm^{-1})	Functional group	Compounds
3600-3200	O-H stretching	EG, EG oligomers, EG derivatives, alcohols, water
3000-2800	C-H stretching	Alkanes
1730-1650	C=O stretching	Carboxylic acids, ketones , aldehydes
1465-1350	C-H bending	Alkanes
1300-950	C-O stretching O-H bending	Alcohols, EG derivatives Phenols, Esters, Ethers
900-750	Aromatic out-of-plane C-H deformation	Aromatics

Table 4: Main signals in the FT-IR spectrum of the oily fraction obtained by solvolytic liquefaction using EG and catalytical amounts of Fe_2O_3/FeOOH nanoparticles.

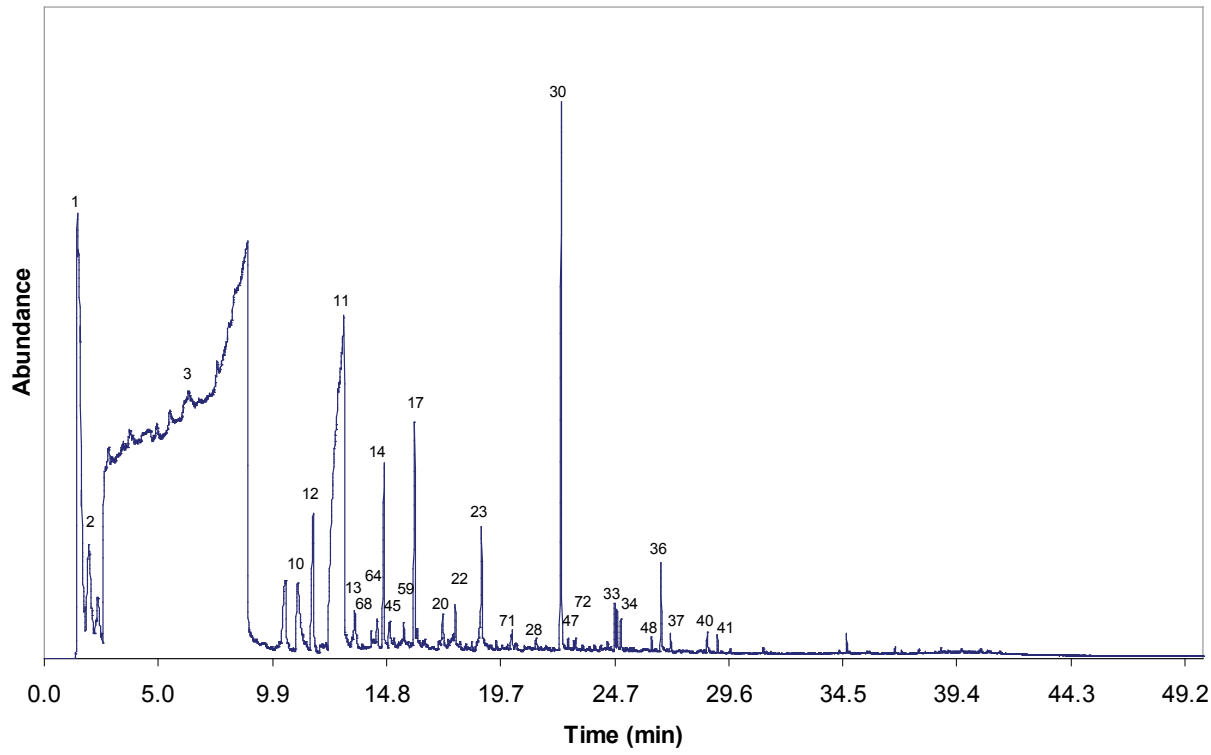

Figure 4: Chromatogram of oil fraction from non-catalytic liquefaction process.

Fe_2O_3/FeOOH nanoparticles, respectively. The pattern and the intensity of the peaks clearly reveal that the composition of both solvolytic oil samples differ significantly. The presence of larger number of compounds is detected in the solvolytic oil fraction that is obtained by catalytic liquefaction. The results show that the presence of catalyst has enhanced the molecular bonds cleavage, and the cracking of EFB fiber into compounds with low molecular weight. The solvolytic oil fraction from non-catalytic liquefaction shows significantly larger amounts of ethylene glycol. In the presence of the Fe_2O_3/FeOOH nanoparticles, the peaks of EG oligomers (di-, tri-, and tetraethyleneglycol) and EG condensation products with alcohols, phenols and organic acids are detected. Furthermore, in the presence of catalyst, higher amounts of lignin-derived degradation products, namely 4-methyl-, 4-ethyl-, 4-vinyl-, 4-propyl-, 4-(prop-1-enyl)-derivatives of guaiacyl and syringyl formed. Partially, the phenolic lignin decombustion products are found, which correspond to the ethylene glycol ethers (phenol, benzoic acid, guaiacol). A similar trend is observed for the polysaccharide degradation products. Higher yield of polysaccharide degradation products is obtained for that solvolytic oil fraction in the presence of catalyst. The identification of these compounds in the solvolytic oil fractions were determined by GC/MS is listed in Table 5.

The percentage of peak area for each identified oil fraction compounds were quantified and distributed based on chemical functional groups, are summarized in Figure 6. Alcohols are the dominant chemical groups in both non-catalytic and catalytic oil fractions, as the total area (%) were 70.17% and 72.48%, respectively. As can be seen in Figure 4 and 5, majority of alcohols group in non-catalytic oil fraction are from ethylene glycol (Peak 3), and small amount of EG derivatives such as di-, tri- and tetra ethylene glycol. Whereas, huge amount of diethylene glycol (Peak 12) was detected in catalytic oil fraction, together with other alcohols group such as ethylene glycol, tri ethylene glycol, tetra ethylene glycol and EG derivatives, and also 3-pentanol and 2-methyl-3-hexanol from holocellulose decomposition. The increase of diethylene glycol compound in catalytic oil fraction showed that the presence of Fe_2O_3/FeOOH enhanced the reaction between EG molecules through dehydrolysis, releasing free radicals of H^+ and OH^- for the cracking reaction of polysaccharide materials, as shown in Figure 7. Hence, this has increased the amount of furans group from 1.50% to 7.15%. Small amount of acids, hydrocarbons, ketones and aldehydes are detected in both non-catalytic and catalytic oil fraction.

Conclusion

The presence of Fe_2O_3/FeOOH nanoparticles as catalyst in EG-based solvolytic liquefaction of empty fruit bunches significantly increased the yield of both polysaccharide and lignin degradation products in the solvolytic oil fraction at comparatively low temperature (250°C). As the HHV for catalytic liquefaction products were only slightly higher compared to non-catalytic process, further purification and separation of the lower-molecular liquefaction products, such as alcohols, ketones, carboxylic acids, and aromatic compounds (phenol, guaiacyl and syringyl derivatives) would be a good step towards further valorization of the oil fraction.

Acknowledgements

The authors would like to acknowledge the financial supports given by the Ministry of Science, Technology and Innovation of Malaysia (MOSTI) for e-Science Fund Grant (03-01-02-SF0030), Ministry of Higher Education of Malaysia (MOHE) for Fundamental Research Grant (UKM-ST-07-FGRS-0232-2010), National University of Malaysia (UKM) for Research University Operation Grant (UKM-OUP-BTT-29-143/2011), ExxonMobil (M) Research Grant (STGL-012-2008), UKM-DIP-2-12-34 and UKM Outbound Mobility Program. The authors also would

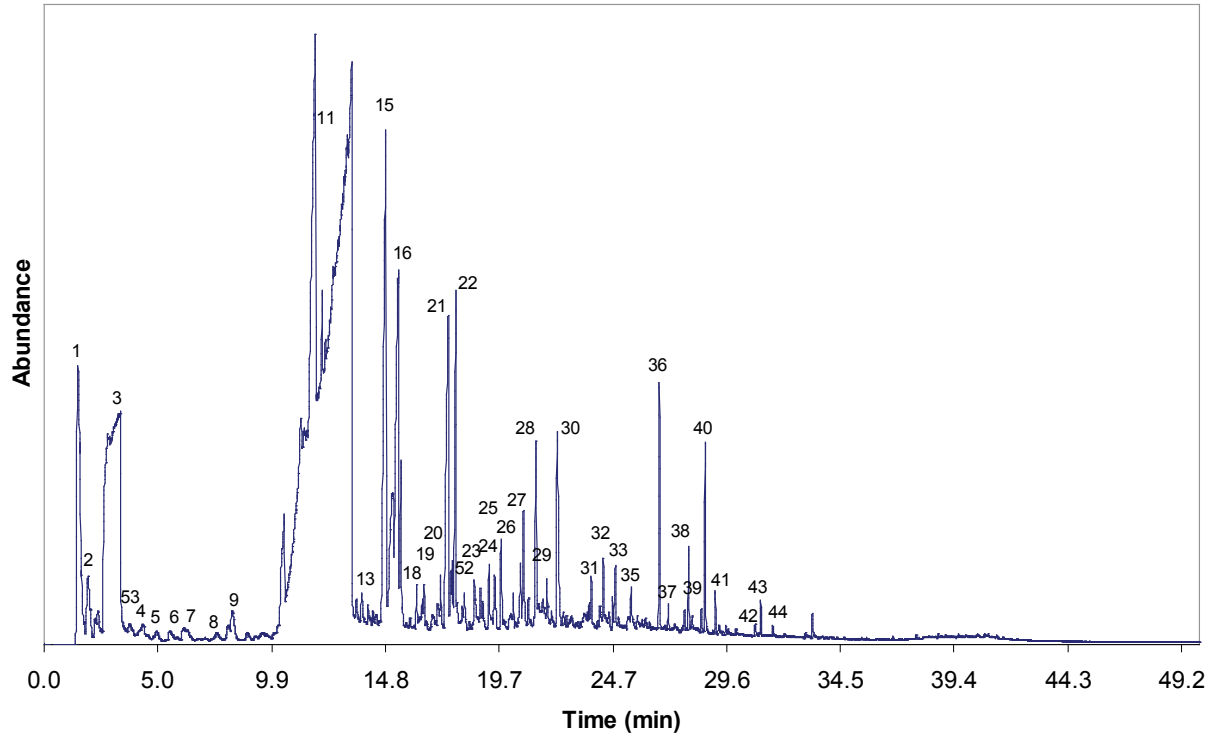

Figure 5: Chromatogram of oil fraction from catalytic liquefaction process.

Peak No.	RT (min)	MW	Compound
1	1.506	44	Carbon dioxide
2	1.993	60	Acetic acid
3	2.640-8.854	62	Ethylene glycol
4	3.756	92	Toluene
5	4.337	162	1,6-anhydro-beta-glucopyranose (levoglucosan)
6	4.931	96	Furfural
7	5.500	112	3-carboxyfurane
8	6.100	104	Ethylene glycol monoacetate
9	7.524		Styrene+carbohydrate derivaties
10	8.201	86	Butyrolactone
11	11.003	94	Phenol
12	11.181 - 13.353	106	Diethylene glycol
13	11.661	114	2-methyl-2-propen-1-ol acetate
14	13.460	108	2-methyl-phenol
15	14.190	116	2-methyl-butanoic acid
16	14.570	76	Propylene glycol
17	14.718	102	2-ethyl-1,3-dioxolane
18	14.843	102	2-ethyl-1,3-dioxolane
19	15.080	76	2-methoxy-ethanol
20	15.383	150	Triethylene glycol
21	15.407	126	3-ethyl-2-hydroxy-2-cyclopenten-1-one
22	16.042	206	2-(2-(2-methoxyethoxy)ethoxy)-acetate ethanol
23	16.172	132	Pentanedioic acid
24	16.499	102	Dipropyl ether
25	17.247	208	Tetraethyleneglycol monomethylether
26	17.537	88	3-pentanol
27	17.787		EG derivaties
28	18.279	174	Diisobutyl acetal
29	18.920	138	2-phenoxy-ethanol
30	19.306	194	Tetraethylene glycol
31	19.549	148	3-methyl-2(3H)-benzofuranone
32	19.828	116	2-methyl-3-hexanol
33	20.208	152	4-ethyl-2-methoxy-phenol
34	20.790	130	3-ethyl-4-hydroxy-dihydro-furan-2-one
35	21.336	102	Tetrahydro-2-furanmethanol
36	21.799	148	1,2,4-trimethoxy-butane
37	22.256	154	2,6-dimethoxy-phenol
38	22.642	166	2-methoxy-4-propyl-phenol
39	22.915	164	1-butyl-4-methoxy-benzene
40	23.710		Guaiacol etherified with EG
41	24.238	166	2-hydroxyethyl benzoate
42	24.761	168	4-methyl-syringol
43	24.915	206	2-methoxy-4-(1-propenyl)-(E)-phenol
44	25.443	146	2,2´-bi-1,3-dioxolane
45	26.245	220	Butylated hydroxytoluene
46	26.654	182	4-ethyl-syringol
47	27.046	180	4-vinyl-syringol
48	27.924		Syringol acid
49	28.476	194	4-prop-1-en-1-yl-syringol
50	28.636	196	4-propyl-syringol
51	29.076	200	1,4-dimethoxy-2,3,5,6-tetramethyl-benzene
52	30.803	194	4,6-dimethoxy-2,3-dimethyl-benzaldehyde
53	31.046	210	4-hydroxy-1,2-benzenedicarboxylic acid, dimethyl ester
54	31.562	182	2,2´-dimethylbiphenyl

Table 5: GC/MS analysis results for the oil fractions obtained in solvolytic liquefaction of EFB, without and in the presence of Fe_2O_3/FeOOH catalyst.

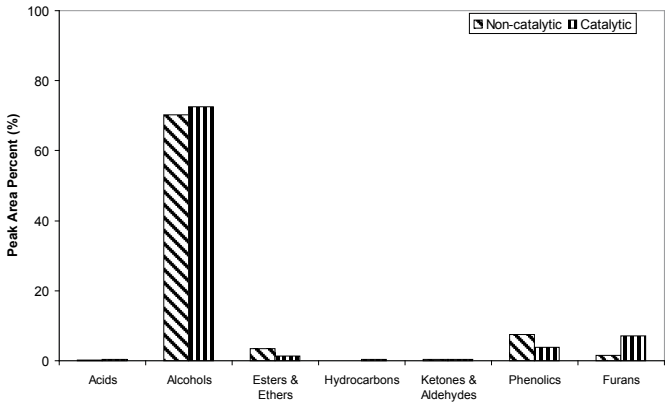

Figure 6: Classification of compound based on chemical functional group in oil fraction obtained from liquefaction of EFB, without and in the presence of FeOOH/Fe_2O_3 catalyst.

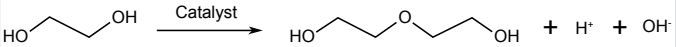

Figure 7: Dehydrolysis of ethylene glycol in the presence of catalyst during solvolytic liquefaction of EFB.

like to acknowledge Department of Chemical, University of Natural Resources and Applied Life Sciences (BOKU), Austria for assistance on Py-GC/MS measurements.

References

1. Alam MZ, Mamun AA, Qudsieh IY, Muyibi SA, Salleh HM, et al. (2009) Solid state bioconversion of oil palm empty fruit bunches for cellulase enzyme production using a rotary drum bioreactor. Biochem Eng J 46: 61-64.
2. Pua FL, Zakaria S, Chia CH, Fan SP, Rosenau T, et al. (2013) Solvolytic liquefaction of oil palm Empty Fruit Bunch (EFB) fibres: Analysis of product fractions Using FTIR and pyrolysis-GCMS. Sains Malays 42: 793-799.
3. Lin L, Yao Y, Yoshioka M, Shiraishi N (2004) Liquefaction mechanism of cellulose in the presence of phenol under acid catalysis. Carbohydr Polym 57: 123-129.
4. Hirano K, Kouzu M, Okada T, Kobayashi M, Ikenaga N, et al. (2001) Catalytic activity of iron compounds for coal liquefaction. Fuel 78: 1867-1873.
5. Karaca H, Ceylan K, Olcay A (2001) Catalytic dissolution of two Turkish lignites in tetralin under nitrogen atmosphere: effects of the extraction parameters on the conversion. Fuel 80: 559-564.
6. Liu Z, Yang J, Zondlo JW, Stiller AH, Dadyburjor DB (1996) *In situ* impregnated iron-based catalysts for direct coal liquefaction. Fuel 75: 51-57.
7. Song C, Saini AK, Yoneyama Y (2000) A new process for catalytic liquefaction of coal using dispersed MoS_2 catalyst generated in situ with added H_2O. Fuel 79: 249-261.
8. Wang G, Li W, Li B, Chen H, Bai J (2007) Direct liquefaction of sawdust under syngas with and without catalyst. Chemical Engineering and Processing: Process Intensification 46: 187-192.
9. Khelfa A, Sharypov V, Finqueneisel G, Weber JV (2009) Catalytic pyrolysis and gasification of *Miscanthus giganteus:* Haematite (Fe_2O_3) a versatile catalyst. J Anal Appl Pyrolysis 84: 84-88.
10. Sharypov VI, Beregovtsova NG, Kuznetsov BN, Baryshnikov SV, Cebolla VL, et al. (2006) Co-pyrolysis of wood biomass and synthetic polymers mixtures: Part IV: Catalytic pyrolysis of pine wood and polyolefinic polymers mixtures in hydrogen atmosphere. J Anal Appl Pyrolysis 76: 265-270.
11. Kaneko T, Tazawa K, Okuyama N, Tamura M, Shimasaki K (2000) Effect of highly dispersed iron catalyst on direct liquefaction of coal. Fuel 79: 263-71.
12. Zhu J, Yang J, Liu Z, Dadyburjor DB, Zhong B, et al. (2001) Improvement and characterization of an impregnated iron-based catalyst for direct coal liquefaction. Fuel Processing Technology 72: 199-214.

13. Kaneko T, Sugita S, Tamura M, Shimasaki K, Makino E, et al. (2002) Highly active limonite catalysts for direct coal liquefaction. Fuel 81: 1541-159.

14. Rezzoug SA, Capart R (2002) Liquefaction of wood in two successive steps: solvolysis in ethylene-glycol and catalytic hydrotreatment. Applied Energy 72: 631-644.

15. Pua FL, Chia CH, Zakaria S, Liew TK, Yarmo MA, et al. (2010) Preparation of transition metal sulfide nanoparticles *via* hydrothermal route. Sains Malays 39: 243-248.

16. Chia CH, Zakaria S, Farahiyan R, Liew TK, Nguyen KL, et al. (2008) Size-controlled synthesis and characterization of Fe_3O_4 nanoparticles by chemical coprecipitation method. Sains Malays 37: 389-394.

17. Demirbaş A (1997) Calculation of higher heating values of biomass fuels. Fuel 76: 431-434.

18. Qian Y, Zuo C, Tan J, He J (2007) Structural analysis of bio-oils from sub-and supercritical water liquefaction of woody biomass. Energy 32: 196-202.

This article was originally published in a special issue, **Biofuels & their applications** handled by Editor(s). Dr. Kirill I Kostyanovskiy, Texas Agri Life Research & Extension Center, USA